

DYNAMIC CENTRIFUGE STUDY OF SEISMICALLY INDUCED LATERAL EARTH PRESSURES

Linda ALATIK¹ and Nicholas SITAR²

ABSTRACT

Seismically induced lateral earth pressures are becoming an important factor in the design of retaining structures and basement walls in seismically active areas. Methods currently in use for evaluating the seismically induced lateral earth pressures gradually evolved from the seminal Japanese work performed in the 1920's. These methods are based on a combination of small scale laboratory model testing and analytical solutions, and usually result in significant seismic design loads. The economic impact of such designs for long retaining structures along rail and road corridors can be substantial and there is a strong incentive to develop effective and economical designs. Therefore, a series of dynamic centrifuge tests aimed at evaluating the magnitude and distribution of seismically induced lateral earth pressures on retaining structures and basement walls is currently underway. Here we present the results of a series of experiments on two retaining structures with dry medium dense sand backfill. Preliminary results indicate that seismically induced lateral earth pressures measured during the experiment are significantly less than those estimated using the most current design methods.

Keywords: seismic, earth pressure, retaining wall, basement wall, centrifuge study

INTRODUCTION

The problem of seismically induced lateral earth pressures on retaining structures and basement walls has received significant attention from researchers over the years. The pioneering work was performed in Japan following the great Kanto Earthquake of 1923 by Okabe (1926) and Mononobe and Matsuo (1929). The method proposed by these authors and currently known as the Mononobe-Okabe (M-O) method is based on Coulomb's theory of static soil pressures. The M-O method was originally developed for gravity walls retaining cohesionless backfill materials and is today, with its derivatives, the most common approach to determine seismically induced lateral earth pressures. Later studies provided design methods mostly based on analytical solutions assuming ideal cohesionless backfill or experimental data from relatively small scale shaking table experiments. Whereas controversy remains on the position of the point of application of the resultant dynamic earth pressure, many researchers have agreed that the M-O method gives adequate results (e.g. Prakash & Basavanna, 1969, Seed & Whitman, 1970, Clough & Frigaszy, 1977, Bolton & Steedman, 1982, Sherif et al., 1982, Ortiz et al., 1983). Recently, however, there have been claims that the M-O method may lead to unconservative estimates of the dynamic earth pressures (e.g. Richards & Elms, 1979, Morrison & Ebeling, 1995, Green et al., 2003, Ostadan & White, 1998, Ostadan, 2004).

¹ PhD Student, Department of Civil & Environmental Engineering, University of California, Berkeley, CA, Email: l_atik@berkeley.edu

² Professor, Department of Civil & Environmental Engineering, University of California, Berkeley, CA.

EXPERIMENTAL SETUP

The centrifuge experiment described in this paper was performed on the 400g-ton dynamic centrifuge at the Center for Geotechnical Modeling at the University of California, Davis. The centrifuge has a radius of 9.1m, a maximum payload of 4,500Kg, and an available bucket area of 4m². The shaking table has a maximum payload mass of 2,700Kg and a maximum centrifugal acceleration of 80g. Additional technical specifications for the centrifuge and the shaking table are available in the literature (Kutter et al., 1994, Kutter, 1995). The centrifugal acceleration used in this experiment was 36g. All test results are presented in terms of prototype units unless otherwise stated.

The model configuration is shown in Figure 1 in model units. The model was constructed in a rectangular flexible shear beam container with internal dimensions of 1.65m long by 0.79m wide by

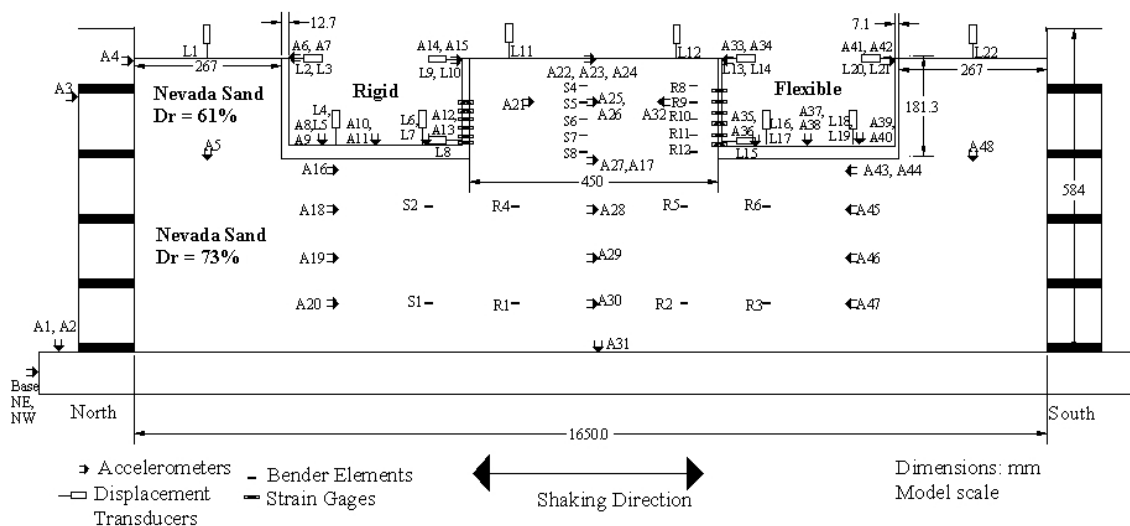


Figure 1. Model configuration, profile view

approximately 0.58m deep. The bottom of the container is coated with grains of coarse sand and is uneven. The container consists of a series of stacked aluminum rings separated by neoprene rubber.

To minimize boundary effects, the container is designed such that its natural frequency is less than the initial natural frequency of the soil (Kutter, 1995).

In prototype scale, the model consists of two retaining wall structures, rigid and flexible, of approximately 6m height spanning the width of the container. The structures have the stiffness, mass and natural frequency of typical reinforced concrete structures. They sit on approximately 12.5m of dry medium dense sand ($D_r = 73\%$) and the backfill soil consists of dry medium dense sand ($D_r = 61\%$). The “rigid” structure was designed to have a top deflection of less than 0.004 the height of the wall during loading. Both structures have rigid mat foundations.

Soil Properties

Nevada sand, a fine, uniform, angular sand, was used in this experiment. Nevada sand has a mean grain size of 0.14 to 0.17mm, a uniformity coefficient of 1.67, and a specific gravity of 2.67 (Kammerer et al., 2000). The minimum and maximum dry densities determined at the University of California, Davis using the Japanese standard method yielded 14.50 and 17.49KN/m³ respectively. The initial friction angle value for the Nevada sand at 61% relative density is 35° (Arulmoli et al., 1992).

Model Preparation

The sand was placed using dry pluviation in five layers underneath the structures and in five layers behind the structures. The height of each layer corresponds to a horizontal array of instruments, as shown in Figure 1. The different soil densities were produced by changing the drop height, mesh opening and speed of drop for the pluviator. After placement of each layer, the sand surface was smoothed with a vacuum and instruments were placed at specific positions. Industrial grease was placed between the structures’ walls and the container to provide a frictionless boundary and prevent sand from passing through.

Instrumentation

The models were densely instrumented in order to collect accurate and reliable measurements of accelerations, displacements, shear wave velocities, strains, bending moments and earth pressures. Horizontal and vertical accelerations in the soil and on the structures were measured using miniature ICP and MEMs accelerometers. Soil settlement and structures’ deflection and settlement were measured at different locations using a combination of LVDTs and linear potentiometers. Shear wave velocities in the soil underneath and behind the structures were measured using bender elements. The locations of accelerometers, bender elements and displacement transducers are shown in Figure 1.

Accurate measurement of lateral earth pressure distribution was the major goal of this study. Stress distribution measurements in laboratory experiments are traditionally achieved using pressure cells. Such measurements are generally inaccurate and non-repeatable due to problems such as cell/soil reaction function of the relative stiffness of the cell with respect to the soil, and inclusion or arching effects caused by the disturbance of the stress field by the presence of the cell (Dewoolkar et al., 2001). In order to avoid these problems, lateral earth pressures were measured using flexible tactile pressure Flexiforce sensors. The Flexiforce sensors, manufactured by Tekscan, are approximately 0.2mm thick. Their sensing area consists of conductive material separated by semi-conductive ink. Lateral earth pressures were also calculated by differentiating the bending strains measured by the strain gages. Direct measurements of the total bending moments at the bases of the walls were measured using force sensing bolts at the wall/foundation joints. The locations of the strain gages, Flexiforce sensors and force sensing bolts on the south rigid and north flexible walls are shown in Figure 2.

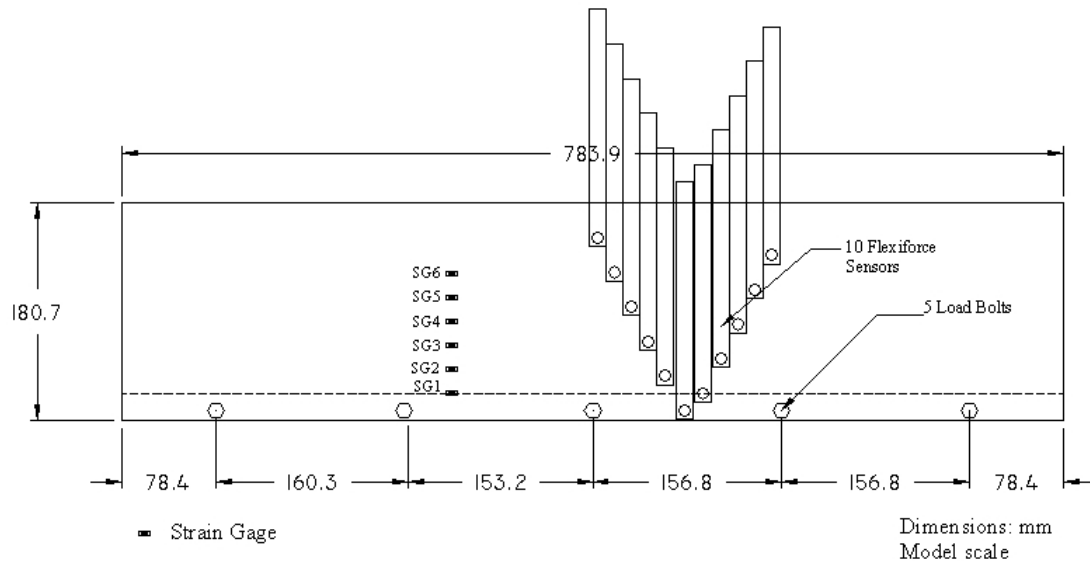


Figure 2. Flexiforce, strain gages and force sensing bolts layout on south rigid and north flexible walls

Shaking Events

Five shaking events were applied to this model in flight at 36g centrifugal acceleration. The shaking was applied parallel to the long sides of the model container. The shaking events consisted of a step wave, a ground motion recorded at the Santa Cruz station during the Loma Prieta earthquake and applied three times to the model, and a ground motion recorded at 80m depth at Port Island during the 1995 Kobe earthquake. The shaking events along with their prototype maximum base peak accelerations are shown in Table 1.

Table 1. Shaking sequence

Shaking Event	Prototype Base Peak Acceleration (g)
Step Wave	0.06
Loma Prieta	0.29
Loma Prieta	0.42
Kobe	0.75
Loma Prieta	0.41

EXPERIMENTAL RESULTS

Acceleration Time Histories

Acceleration time histories were collected at the accelerometer locations shown in Figure 1. The acceleration time histories were used in evaluating the amplification and deamplification of the input ground motions, and in evaluating the magnitude of seismically-induced forces. Figure 2 shows the peak accelerations measured at the base of the container versus those measured at the top of the soil, south rigid wall, and north flexible wall during the different shaking events. A 45° line is displayed for reference.

It is apparent that the amplification during initial events is consistently higher than during later events. While the motions are consistently amplified at the top of the walls, the acceleration at the top of the soil crosses over the 45° line indicating attenuation due to the large magnitude of the shaking event.

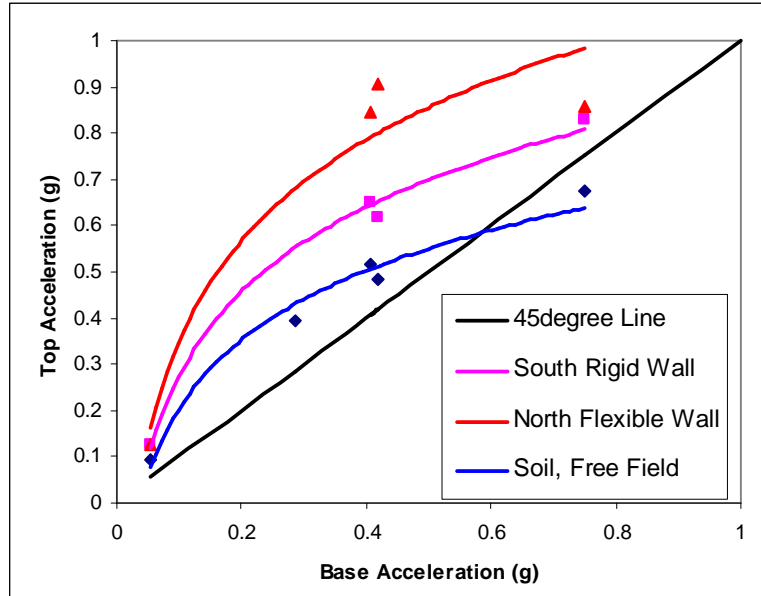


Figure 3. Base motion amplification/deamplification for the soil, rigid and flexible structures

Soil Settlements

Vertical soil deformation measurements were taken at the soil surface and at the structures' foundations as shown in Figure 1. The static offsets measured by the displacement transducers were used to determine the total settlement of the backfill soil as well as the soil underneath the structures (base soil) after the different shaking events. Table 2 shows these settlement values along with the relative density of the soil after each shake. It is apparent that the maximum total settlement happened after the Kobe event due to larger magnitude of shaking, hence greater soil densification.

Table 2. Total soil settlement after different shaking events

Shaking Event	Settlement (mm)		Relative Density (Dr %)	
	Base Soil	Backfill	Base Soil	Backfill
Step Wave	0.32	0.52	74.37	61.75
Loma Prieta 1	31.55	22.46	75.65	63.54
Loma Prieta 2	18.17	2.14	76.38	63.70
Kobe	37.56	37.3	77.91	66.70
Loma Prieta 3	4.47	5.49	78.08	67.08
Total	92.06	67.91		

Moment Distributions

The south rigid and north flexible walls were instrumented with five force sensing bolts and six strain gages each, as shown in Figure 2. The moment distributions along the heights of the walls were calculated based on the strain values measured by the strain gages. The total dynamic moment distributions on the south rigid and north flexible walls are shown in Figure 3 for the different shaking events. It is apparent that the total dynamic moments on the flexible wall are consistently about half those on the rigid wall. Moreover, the total dynamic moments decreased for the second and third Loma Prieta motion due to the soil's densification. The maximum total dynamic moments occurred during the Kobe motion due to the large magnitude of shaking.

The moment distributions along the bases of the walls were directly measured by the force sensing bolts and interpreted from the strain gages data. Table 3 shows the total dynamic moments at the bases of the south rigid and north flexible walls interpreted from the strain gage data and measured by the force sensing bolts during the different shaking events. The total dynamic moments estimated using

the M-O pressure distribution with the total resultant force applied at one third the height of the wall from its base are presented for comparison in Table 3. The total dynamic moments estimated using the Seed & Whitman (1970) method with the resultant force of the dynamic increment applied at two thirds the height of the wall from its base are also presented in Table 3. The M-O and Seed & Whitman (1970) total dynamic moments were estimated using the peak ground acceleration as well as 85% and 65% of the peak ground acceleration measured by accelerometer A22, shown in Figure 1, at the soil surface in the free field.

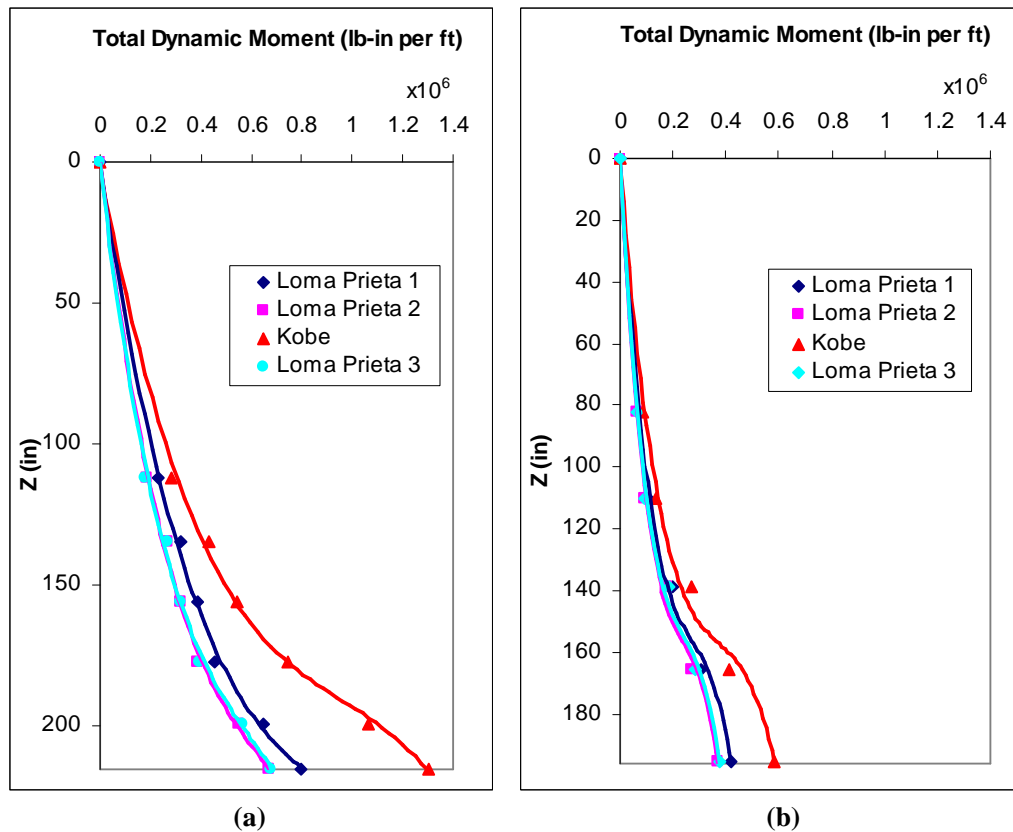


Figure 4. Total dynamic moment distributions measured on (a) rigid and (b) flexible walls by strain gages

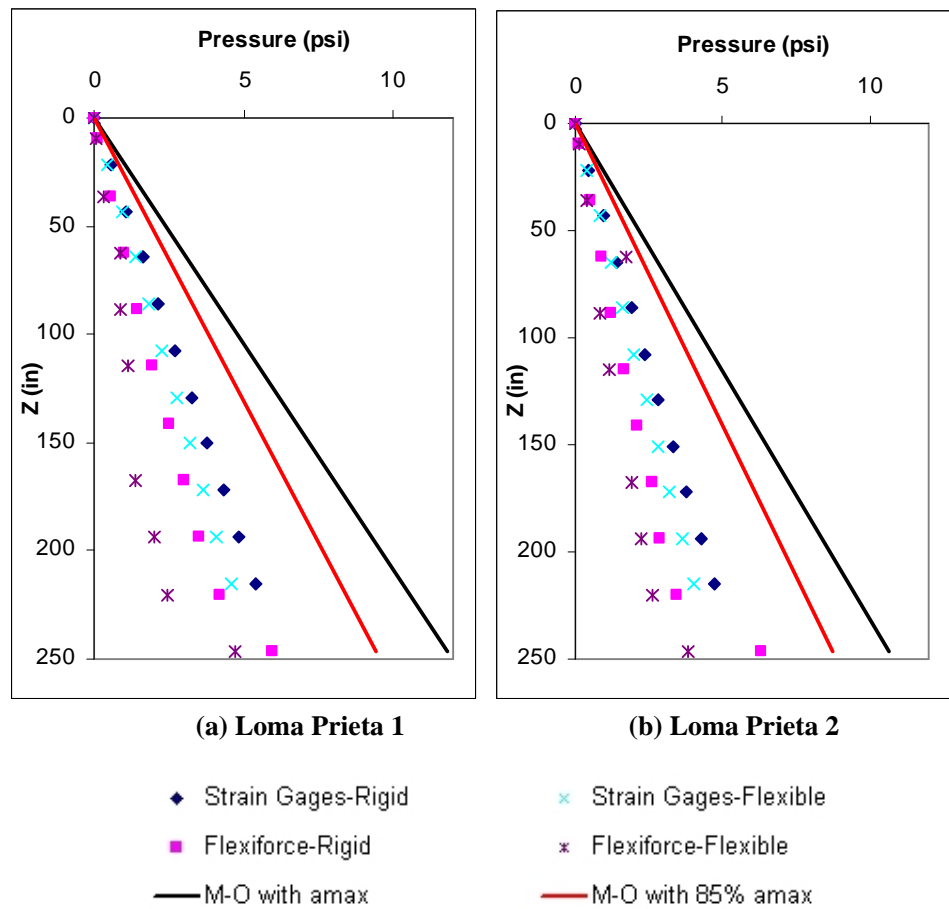
Table 3. Total dynamic moments at the bases of the south rigid and north flexible walls

		Total Dynamic Moments at the Base (lb-in)			
		Loma Prieta 1	Loma Prieta 2	Kobe	Loma Prieta 3
Strain Gages	Rigid	9.26E+07	7.87E+07	1.60E+08	8.07E+07
	Flexible	6.74E+07	5.90E+07	9.49E+07	6.07E+07
Force Sensing Bolts	Rigid	9.51E+07	1.03E+08	1.77E+08	1.00E+08
	Flexible	3.12E+07	3.41E+07	6.19E+07	3.56E+07
M-O Method with a_{max}		1.23E+08	1.11E+08	2.41E+08	1.17E+08
M-O Method with 85% a_{max}		9.76E+07	9.03E+07	1.48E+08	9.75E+07
Seed and Whitman (1970) Method with a_{max}		1.49E+08	1.42E+08	1.82E+08	1.48E+08
Seed and Whitman (1970) Method with 65% a_{max}		1.11E+08	1.07E+08	1.33E+08	1.10E+08

The data in Table 3 show that the M-O and Seed & Whitman (1970) methods using the peak ground acceleration values consistently overestimate the total dynamic moment values. The total dynamic moments observed for the rigid and flexible walls are approximately 65 to 75% and 40 to 55% of the values estimated by the M-O method, respectively. The total dynamic moments observed for the rigid and flexible walls are approximately 50 to 60% and 40 to 50% of the values estimated by the Seed & Whitman (1970) method, respectively. Using 85% and 65% of the peak ground acceleration in the M-O and Seed & Whitman methods respectively seems to be more reasonable in estimating the total dynamic moments applied at the base of the rigid wall but still overestimates the total dynamic moments applied at the base of the flexible wall.

Lateral Earth Pressures

Ten Flexiforce sensors were mounted on all four walls at the locations shown in Figure 2 to directly measure the seismically induced lateral earth pressures. We observed a consistent agreement between the dynamic earth pressures measured at the north and south walls of each structure. Figure 5 shows the total dynamic pressure distributions on the rigid and flexible walls during the different shaking events. The pressure distributions estimated by the M-O method using the peak ground acceleration and 85% of the peak ground acceleration are displayed for comparison.



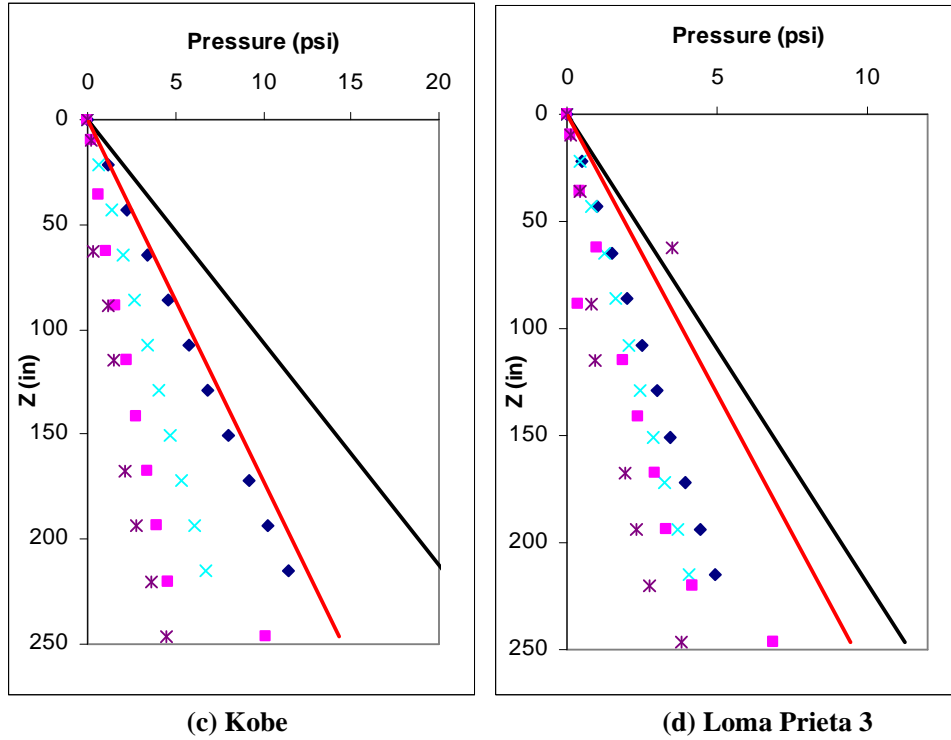


Figure 5. Total dynamic pressure distributions on the south rigid and north flexible walls during the (a) Loma Prieta 1, (b) Loma Prieta 2, (c) Kobe, and (d) Loma Prieta 3 shaking events

The pressures measured by the Flexiforce sensors were generally in good agreement with those interpreted by double differentiating the strain gage measurements. It is apparent in Figure 5 that the total dynamic pressure distributions measured on the rigid and flexible walls are respectively about 45 to 50% and 30 to 40% the pressures estimated by the M-O method using the peak ground acceleration, with the exception of those observed on the rigid wall during the Kobe motion.

CONCLUSION

We present the preliminary results of the first in a series of centrifuge experiments on the evaluation of the magnitude and distribution of seismically induced lateral earth pressures on retaining structures and basement walls. Results of these centrifuge experiments indicate that the seismically induced lateral pressures of a medium dense sand backfill appear to be overestimated by currently used design methods. The magnitude of the total dynamic earth pressures is about 45 to 50% and 30 to 40% of the values estimated by the M-O method using the peak ground acceleration for a rigid and a flexible wall respectively. For design purposes, we show that the total dynamic moments at the bases of a rigid and flexible wall are about 50 to 60% and 40 to 50% of the values calculated applying the Seed & Whitman (1970) method with the peak ground acceleration and the dynamic component's resultant located at two thirds the height of the wall from its base.

Using 85% of the peak ground acceleration with the M-O method and 65% of the peak ground acceleration with the Seed & Whitman (1970) method yields predictions of the total dynamic pressures and moments that are closer the actual values measured during the experiment.

ACKNOWLEDGEMENTS

The authors gratefully acknowledge the contributions and suggestions provided by Prof. Bruce Kutter, Dr. Dan Wilson and all the staff at the University of California, Davis Center for Geotechnical Modelling. This work was supported by a grant from the Bay Area Rapid Transit (BART) and the Santa Clara Valley Transportation Authority (VTA) to the Pacific Earthquake Engineering Research Center at UC Berkeley. The authors gratefully acknowledge the support provided by Ed Matsuda at BART and James Chai at VTA.

REFERENCES

- Arulmoli, K, Muraleetharan, KK, Hosain, MM, and Fruth, LS. "VELACS Laboratory Testing Program, Soil Data Report," The Earth Technology Corporation, Irvine, California, Report to the National Science Foundation, Washington D.C., March, 1992.
- Bolton MD, and Steedman, RS. "Centrifugal testing of micro-concrete retaining walls subject to base shaking," Proceedings of Conference on Soil dynamics and Earthquake Engineering, Southampton, 1, 311-329, Balkema, 1982.
- Dewoolkar, MM, Ko, H, and Pak RYS. "Seismic Behavior of Cantilever Retaining Walls with Liquefiable Backfills," Journal of Geotechnical and Geoenvironmental Engineering, ASCE, 127-5, 424-435, 2001.
- Green, RA, Olgun, CG, Ebeling, RM, and Cameron, WI. "Seismically Induced Lateral Earth Pressures on a Cantilever Retaining Wall," Earthquake Engineering, 2003.
- Kammerer, AM, Wu, J, Pestana, JM, Riemer, M, and Seed, RB. "Cyclic Simple Shear Testing of Nevada Sand for PEER Center Project 2051999," Geotechnical Engineering Report No. UCB/GT/00-01, University of California, Berkeley, CA, 2000.
- Kutter, BL, Idriss, IM, Kohnke, T, Lakeland, J, Li, XS, Sluis, W., Zeng, X, Tauscher, RC, Goto, Y, and Kubodera, I. "Design of a Large Earthquake Simulator at UC Davis," Centrifuge 94, Leung, Lee, and Tan (eds.), Balkema, 169-175, 1994.
- Kutter, BL. "Recent Advances in Centrifuge Modeling of Seismic Shaking," Proceedings., 3rd International Conference on Recent Advances in Geotechnical Earthquake Engineering and Soil Dynamics, St. Louis, Vol. II, 927-941, 1995.
- Mononobe N, Matsuo M. "On the determination of earth pressures during earthquakes," Proceedings, World Engineering Congress, Vol. 9, 179-187, 1929.
- Morrison, EE, and Ebeling, RM. "Limit equilibrium computation of dynamic passive earth pressure," Canadian Journal of Geotechnical Engineering, Vol. 32, 481-487, 1995.
- Okabe S. "General theory of earth pressure," Journal of the Japanese Society of Civil Engineers, Tokyo, Japan, Vol. 12, No. 1, 1926.
- Ortiz, LA, Scott, RF, and Lee, J. "Dynamic centrifuge testing of a cantilever retaining wall," Earthquake Engineering and Structural Dynamics, Vol. 11, 251-268, 1983.
- Ostadan, F, and White, WH. "Lateral Seismic Earth Pressure an Updated Approach," US-Japan SSI Workshop, USGS, Menlo Park, CA, 1998.
- Ostadan, F. "Seismic Soil Pressures for Building Walls an Updated Approach," 11th International Conference on Soil Dynamics and Earthquake Engineering (11th ICSDEE) and the 3rd International Conference on Earthquake Geotechnical Engineering (3rd ICEGE), University of California, Berkeley, 2004.
- Prakash, S. and Basavanna, B.M. "Earth pressure distribution behind retaining wall during earthquakes," Proceedings of the Fourth World Conference on Earthquake Engineering, Santiago, Chile, 1969.
- Richards, R, and Elms, DG. "Seismic behavior of gravity retaining walls," Journal of the Geotechnical Engineering Division, ASCE, 105, (GT4), 449-64, 1979.
- Scott, RF. "Centrifuge Modeling and Technology: A Survey," Revue Francaise de Geotechnique, 48, 15-34, 1998.

- Seed, HB, and Whitman, RV. "Design of earth retaining structures for dynamic loads," Lateral stresses in the ground and design of earth retaining structures, ASCE, New York, 103–147, 1970.
- Sherif, MA, Ishibashi, I, and Lee, CD. "Earth pressure against rigid retaining walls", Journal of Geotechnical Engineering, ASCE, 108, 679-695, 1982.
- Sitar, N. "Geotechnical Reconnaissance of the Effects of the January 17, 1995, Hyogoken-Nanbu Earthquake, Japan," Earthquake Engineering Research Center, University of California, News, Vol. 16, No. 4, October, 1995.
- Stadler AT. "Dynamic centrifuge testing of cantilever retaining walls," PhD thesis, University of Colorado at Boulder, August 1996.